JOM, Vol. 72, No. 4, 2020
https://doi.org/10.1007/s11837-020-04053-3

TECHNICAL ARTICLE

Highly Efficient Beneficiation of Low-Grade Iron Ore via Ore–Coal Composite-Fed Rotary Kiln Reduction: Pilot-Scale Study

RONGHAI ZHONG,[1] LINGYUN YI,[1,2] ZHUCHENG HUANG,[1] WEI CAI,[1] and XIONG JIANG[1]

1.—School of Minerals Processing and Bioengineering, Central South University, Changsha 41-0083, Hunan, China. 2.—e-mail: ylycsu@126.com

Direct reduction of low-grade iron ore pelleted with coal was investigated using a pilot-scale rotary kiln. The evolution of the iron minerals, the strength of the pellets, and the emission characteristics were measured. The results showed that the rotary kiln could be divided into three major functional zones: reduction of hematite to wüstite occurred at 1023–1163 K; wüstite transformed to fine metallic iron particles at 1163–1318 K; and metallic iron particles aggregated within 6.5 m of the outlet. The product had a metallization ratio of 92%. Pellet strength was maintained at 30–45 N within the first zone and no disintegration occurred. Aggregation of metallic iron particles within the final zone improved the strength to 465 N. The reduced sample was treated by grinding followed by magnetic separation. Of the total iron in the ore, 85.61% was recovered as iron powder (grade: 92.0 mass%). Use of this process could reduce CO_2 emissions by approximately 10%.

INTRODUCTION

Gradual depletion of high-grade iron ores necessitates the utilization of refractory low-grade iron ores.[1,2] Refractory iron ores, which are characterized by low iron [total iron (TFe) ≤ 40 mass%] and high SiO_2 content (≤ 50 mass%), fine target mineral grains (average size < 0.045 mm), and complex mineralogy, are widely distributed.[3–5] Efficient utilization of such resources is still a challenge.[6–8]

Coal-based direct reduction followed by magnetic separation has generally been applied for the treatment of these ores.[2,4,9–14] Iron oxides can be reduced to pure metallic iron and then separated from the ores by magnetic separation. Products with a degree of metallization exceeding 85% can be obtained from raw ores (TFe 43.18–47.66 mass%, SiO_2 17.0–49.5 mass%) that were direct-reduced at 1373–1523 K for 60–100 min,[2,4,9,10,12] from which 80% of the iron content could be recovered in the form of iron powder (TFe ≥ 90%) by grinding followed by magnetic separation. However, these laboratory studies recommend a high reduction temperature range, which is impractical for commercial production. One of the biggest obstacles to popularizing the application of this technique is the lack of an industrialized solution and quantitative pilot-scale test data.[15]

Research indicates that three principal factors are beneficial for improving reducibility:[16,17] small diameter, coal blending, and a suitable distribution of pore diameters for gas diffusion. Accordingly, our research group proposed an integrated direct-reduction technology to treat a typical low-grade ore.[18–20] Composite pellets (CPs), prepared from a raw ore (TFe 33 mass%, SiO_2 40 mass%) and coal, were reduced at 1223–1263 K for 35–60 min to obtain samples with a degree of metallization exceeding 80%. Subsequent magnetic separation produced concentrates (TFe ≥ 80 mass%) with a recovery of 80%. To popularize this low-temperature rapid-reduction technology, a pilot-scale test was carried out.

The present work focuses on the direct reduction of low-grade iron ore–coal CPs in a pilot-scale rotary kiln (RK; Φ 1.5 m × 15 m), with the aim of seeking a possible alternative route for the beneficiation of low-grade iron resources. The evolution of the iron minerals, the strength transformation of the CPs,

(Published online February 14, 2020)

and the emission characteristics during the RK reduction process were investigated in situ based on the pilot-scale running conditions.

MATERIALS AND METHOD

Materials

A typical low-grade iron ore (TFe 33.86 mass%, SiO_2 40.61 mass%) was obtained from the Qidong area (Hunan province, China). Its other constituents included 4.36 mass% Al_2O_3, 1.57 mass% CaO, 1.58 mass% K_2O, and 1.05 mass% MgO. X-ray diffraction (XRD) (Fig. 1a) showed that hematite and quartz comprised the dominant phases. Scanning electron microscopy (SEM) (Fig. 1b) showed that fine hematite grains were embedded in a complex relationship with the gangue. Bituminous coal, comprising 58.53 mass% fixed carbon, 31.46 mass% volatile matter, and 10.01 mass% ash, was used as the reducing agent.

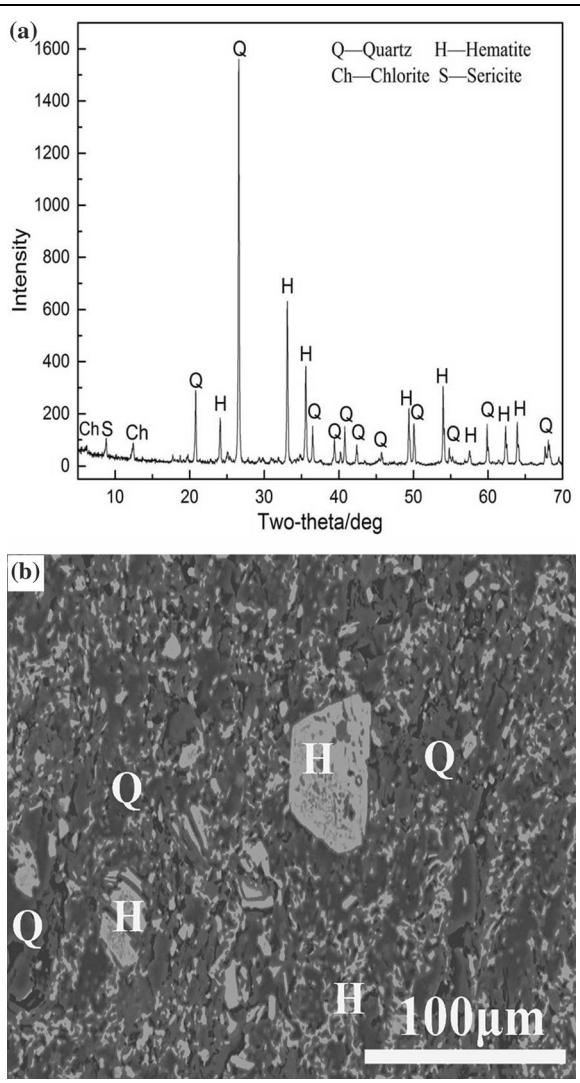

Fig. 1. Mineralogical analyses of iron ore. (a) X-ray diffraction pattern and (b) scanning electron microscopy image. Q quartz; H hematite

Method

The pilot-scale reduction flowsheet included grinding, pelletizing, drying, RK reduction, and cooling procedures (as shown in Fig. 2). Raw ore and coal were milled to 70 mass% < 0.037 mm, then a mixture of iron ore powder (82.19 mass%), coal powder (16.81 mass%), and bentonite (1.0–1.5 mass%) were pelletized into CPs using a disc pelletizer (diameter 2 m, inclination angle 45°, rotational speed 26 rpm). Green CPs (diameter: 3–8 mm) were dehydrated in a cylindrical drier (flue gas discharged from the RK was the inlet for the drying medium). Dried CPs were fed into the RK (Φ 1.5 m × 15 m) for reduction for a duration of 100 min. The reduced sample (metalized pellets and residual coal) were discharged from the RK head and cooled to room temperature in a cylindrical cooler. The metallized pellets were separated from the residual coal by a magnetic drum for subsequent iron beneficiation.

Reduction of CPs was carried out in the RK shown in Fig. 2. CPs and extra coal were fed into the end of the RK and the reduced products were discharged from the head. Injection coal was jetted into the RK at 618 kg/h via a gun from the kiln head. Combustion air was blown in through five air pipelines (total flow quantity of 2120 m^3/h). Throughput was 786 kg reduced pellets and 410 kg residual coal per hour. The temperature distribution along the RK was measured in real time by seven built-in thermocouples. After the RK had run under stable conditions for several weeks, the burden materials were cooled to room temperature in a N_2 atmosphere and sampled at intervals of 0.5 m along its length for characterization. The metallization ratio was employed to evaluate the degree of reduction of the CPs, shown in Eq. 1:

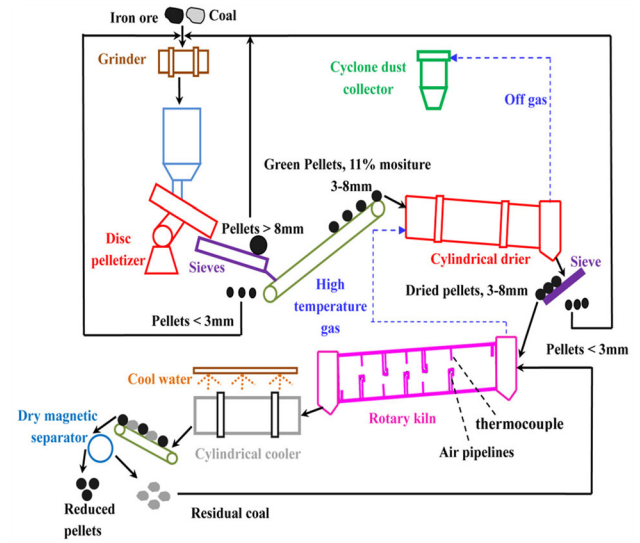

Fig. 2. Schematic diagram of pilot-scale reduction equipment

$$\text{Metallization ratio}\,(\%) = \frac{\text{MFe}}{\text{TFe}} \times 100 \qquad (1)$$

where TFe and MFe are the total iron and metallic iron contents of a sample, respectively.

The compressive strength of the sampled CPs was tested by an intelligent strength-measuring instrument. Their pore size distribution was measured using the Barrett–Joyner–Hallender (BJH) method. Phase transitions were analyzed by XRD using a Cu-Kα source operated at 40 kV and 250 mA (D/max 2550PC; Rigaku, Japan). Microstructural transformation was observed by SEM (JSM-6490LV; JEOL, Japan).

RESULTS AND DISCUSSION

Reduction Behavior of Composite Pellets in Rotary Kiln

Evolution of the CPs during the RK reduction process was analyzed according to the methods described in "Method" section. The results are shown in Fig. 3.

Figure 3(a) shows that the FeO content in the CPs increased sharply within the 13.5- to 11.0-m zone (distance to RK head). Only 2 mass% FeO was detected in CPs at the 13.5-m position; this value surged to 17.45 mass% at 11.0 m. The corresponding temperature within this zone also showed a steady rise and reached about 1160 K. The FeO contents of the CPs decreased from 11.5 m to 6.5 m owing to the rapid formation of metallic iron. The metallic iron contents in the CPs rose from 1.84 mass% to 24.78 mass%, with a corresponding temperature range of 1163–1318 K. Thereafter, further reduction of iron oxides proceeded weakly until the CPs were discharged via the kiln head. Products with a metallic iron content of 26.85 mass% (metallization ratio of 92.84%) were obtained.

For carbothermal reduction, the reaction rate of reduction by carbon monoxide is much faster than that of solid carbon.[21] Reduction of Fe_2O_3 follows the order $Fe_2O_3 \rightarrow Fe_3O_4 \rightarrow FeO \rightarrow Fe$ when the temperature exceeds 843 K, as shown by Eqs. 2–4:

$$3Fe_2O_3 + CO \rightarrow 2Fe_3O_4 + CO_2 \qquad (2)$$

$$Fe_3O_4 + CO \rightarrow 3FeO + CO_2 \qquad (3)$$

$$FeO + CO \rightarrow Fe + CO_2 \qquad (4)$$

Previous research showed that the reduction of Fe_2O_3 to FeO occurs rapidly, but the reduction of FeO to Fe is always slow, owing to its requirement for a higher reduction potential.[22,23] XRD analysis (Fig. 3b) revealed that most of the Fe_2O_3 phase transformed to Fe_3O_4 or FeO by 11.5 m, indicating that Fe_2O_3 could be reduced to FeO within the 15- to 11-m zone at a relatively lower temperature. Thus,

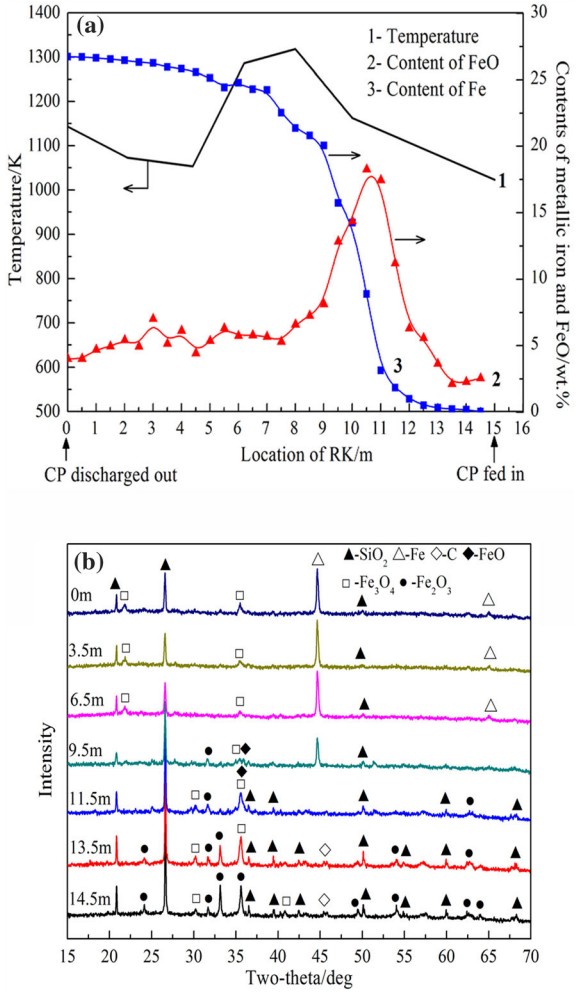

Fig. 3. Transitions of iron oxides in a rotary kiln as a function of distance from the head: (a) metallic iron and FeO contents, and (b) x-ray diffraction patterns

to achieve energy savings, the temperature range in this zone could be appropriately lowered. The high-temperature zone (11–5.5 m) in the RK was beneficial for the transformation of FeO to Fe. In addition to improving the coal reactivity, promotion of the Boudouard reaction by the temperature increase the reduction of FeO was also facilitated.[24] The kinetics of the iron oxide reduction also improved with a rise in temperature. Therefore, the temperature range within the 11- to 7.0-m zone in the RK (mainly for the reduction of FeO to Fe) should be higher. At the kiln head (0 m position), metallic iron and quartz proved to be the major phases present in the discharged CPs.

The results of the analysis of the microstructural evolution of CPs in the RK are shown in Fig. 4. The CPs were mainly composed of three ingredients: gangue, iron minerals, and coal. As the CPs moved to the 11.5-m location of the RK, Fe_2O_3 was reduced to FeO at the periphery (as shown in Fig. 4c), but hematite particles could still be observed in the core (Fig. 4d). At the 9.5-m position, many fine metallic

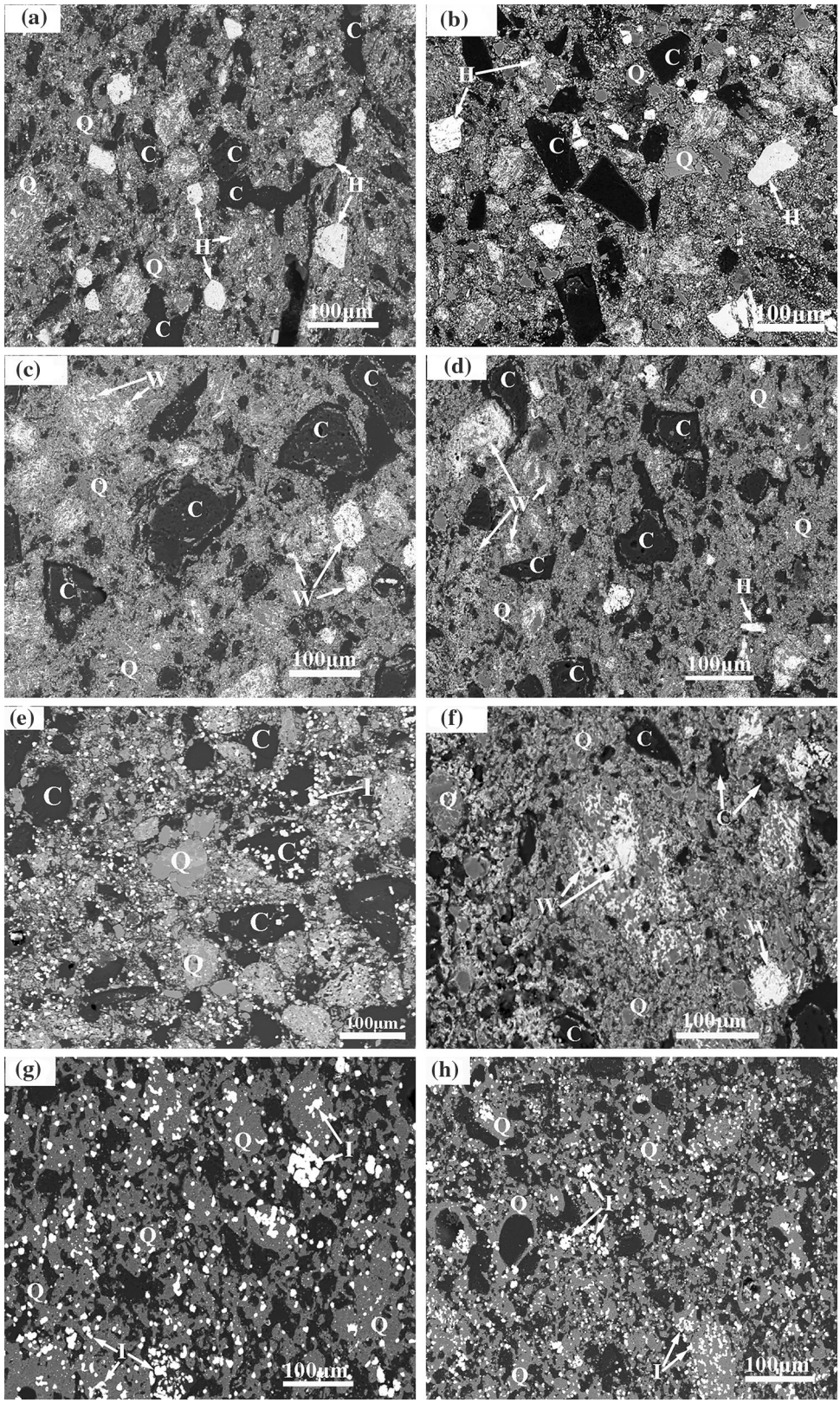

Fig. 4. Scanning electron micrographs of composite pellets at different positions down the length of the rotary kiln. (a), (c), (e), and (g) show microstructures at the peripheries of the pellets; (b), (d), (f) and (h) show the cores. (a), (b) 14.5 m; (c), (d) 11.5 m; (e), (f) 9.5 m; (g), (h) 0 m. H Fe_2O_3; Q SiO_2; C carbon; W FeO

Table I. Concentrates (in mass%) obtained by magnetic separation of reduced pellets

Concentrate yield	TFe	Recovery	MFe
25.60	92.04	85.61	85.63

iron particles began to form at the periphery (Fig. 4e), while FeO remained almost unreduced in the core (Fig. 4f). Fine iron particles then gradually grew into concentrated aggregates (Fig. 4g) at 0 m, which would greatly improve the iron recovery in the subsequent beneficiation process.

From the above discussion, the reduction behavior of low-grade iron ore–coal CPs through the length of the RK could be described as follows: CPs were pre-heated and most Fe_2O_3 was reduced to FeO in the 13.5- to 11.0-m zone; most FeO was rapidly reduced to Fe within the 11.5- to 6.5-m zone; and remaining FeO was further reduced and metallic iron particles aggregated within the 6.5- to 0-m zone.

The results of grinding followed by magnetic separation of the metallized pellets, after milling to 95 mass% < 0.045 mm, are shown in Table I. Concentrates with a high metallization ratio (93.40%) are a desirable raw material for electric arc furnace steelmaking. The RK reduction and subsequent magnetic separation indices indicate that this low-temperature direct-reduction technology is feasible for low-grade iron ore treatment.

Strength Characteristics of Composite Pellets in the Rotary Kiln

Variations in the compressive strength of the sampled CPs along the RK are shown in Fig. 5(a). The compressive strength of CPs within the 14.5- to 11-m zone was maintained at 30–45 N. This value increased rapidly within the 11- to 6.0-m zone and reached 385 N at the 6.0-m position. Hereafter, the strength slowly increased in the 6.0- to 0-m zone, and finally reached 465 N at the kiln head.

During the reduction process, the pore volume change caused by iron mineral transitions may lead to strength loss and disintegration of the pellets.[25,26] The compressive strength of oxidized pellets has been shown to decrease from ~ 3000 N to ~ 550 N during reduction of hematite to wüstite, and then increase to ~ 900 N during metallic iron formation.[27] The thermal strength of iron ore–carbon pellets was reported to drop significantly above 1073 K, but improve for continuous metallic iron crystallization.[28] Coal-fired RKs are widely applied in direct-reduction iron (DRI) production; however, ringing has always been the bottleneck for RK operation, which is primarily attributed to disintegration of the pellets.[29–31] Maintaining the strength of pellets during the reduction process is therefore essential for RK production.

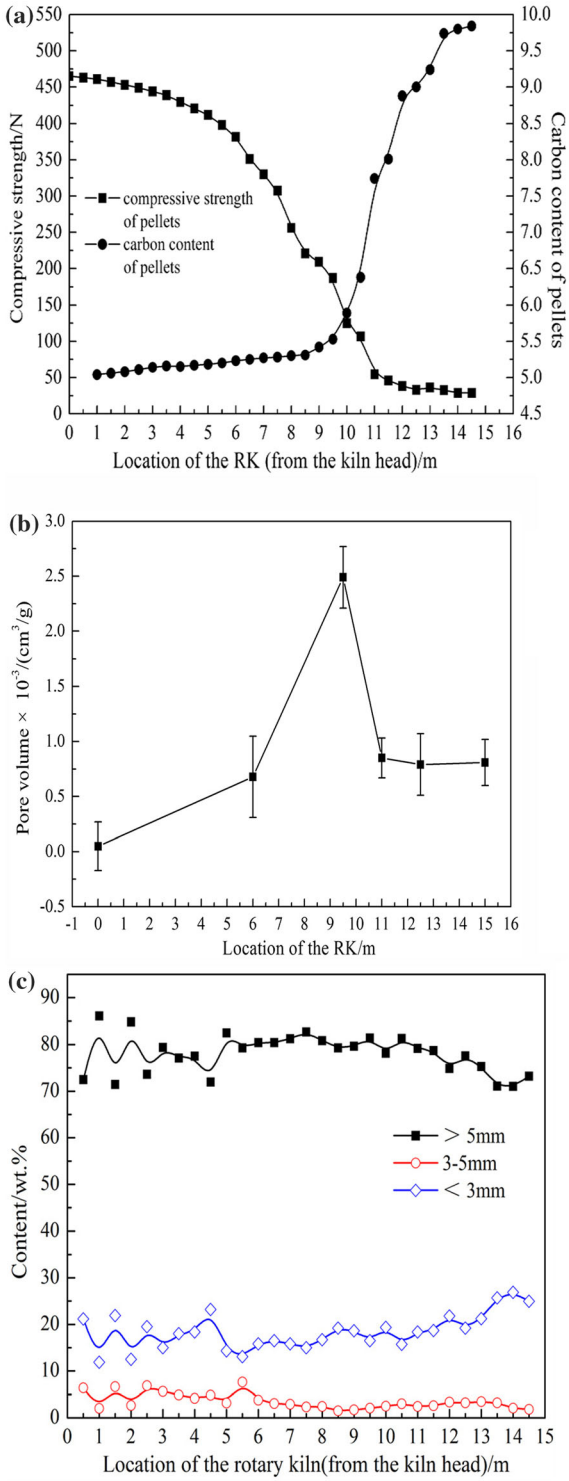

Fig. 5. Strength characteristics of composite pellets as a function of their position in the rotary kiln. (a) Compressive strength and carbon content, (b) pore volume (V_{BJH}) distribution, and (c) particle size distribution

In the present RK reduction process, the strength of the CPs remained stable because large amounts of FeO formed within the 13.5- to 11.5-m zone (Fig. 3a). Pore volume distribution in the CPs is shown in Fig. 5b. The pore volume of CPs at 14.5- to

Table II. Comparison of carbon consumption and CO_2 emissions of rotary kiln reduction processes

Items	Oxidized pellets fed RK reduction[a]	Present technology
TFe in raw iron ore (mass%)	66.7	33.86
Duration (min)	≥ 300	100
Metallization ratio of products (mass%)	95	92
TFe in reduced pellets (mass%)	90.72	28.77
Raw iron ore (kg/t)	1722.49	11,157.98
Carbon (kg/t)	665.57	596.80
Energy consumption of magnetic separation (kg standard coal/t)	–	23.18
CO_2 emissions (kg/t)	2437.99	2186.58

[a]Data from oxidized pellets reduced in a Φ 4.8 m × 80 m rotary kiln (ISCOR, direct reduction plant, South Africa).[36]

11.0-m was maintained between 0.79 cm^3/mg and 0.85 cm^3/mg. This stable pore distribution avoided disintegration or fraction of the CPs. The pore volume then showed an obviously upward trend as coal was consumed in the 11.5- to 9.5-m zone. Metallic iron formed at the periphery of the CPs (as shown in Fig. 4e), so that their strength increased (to 187.9 N), even though a loose structure was observed in their cores (Fig. 4f). Previous research has also indicated that metallic iron formation could improve the strength of pellets during the reduction process.[25,26]

When most FeO had been reduced to Fe, the consumption of coal powder in the CPs dropped. Agglomeration of metallic iron particles led to a decrease in porosity, that is, densification of the CP structure. Accompanying the above change, the compressive strength of the CPs rose to 380 N at the 6.0-m location. At 0 m (kiln head), CPs with a pore volume of 0.0476 cm^3/mg became much more compact, and their corresponding strength increased to 465 N. Size distribution of the CPs remained almost constant along the entire RK length, as shown in Fig. 5c. This indicated that no obvious disintegration or fracture of the CPs occurred during reduction. The ideal strength characteristic of CPs should be self-induration during heating and reduction.[32] During this RK reduction process, aggregation of metallic iron particles and structure densification of CPs probably coincided with the ideal model and therefore avoided disintegration or fracture.

Consumption and Emission Characteristics of Rotary Kiln Process

In China, CO_2 emissions from ironmaking and steelmaking industries account for approximately 10% of total emissions and rank third among all sources.[33,34] More than 60% of CO_2 is produced by ironmaking procedures [sintering, coking, and blast furnace (BF) operation] during BF–basic oxygen furnace processes.[35] For the direct reduction–electric arc furnace route, highly metallized DRI is used for steelmaking, which provides a promising way for reducing CO_2 emissions by omitting coking, sintering, and BF operations. Commercially, the BF process requires 1.75 t iron ore and 0.75 t coke per ton pig iron, accompanied by 2.75 t of CO_2 emissions.[14] The consumption and emission characteristics for the DRI process per ton iron are listed in Table II.

Table II shows that, for oxidized pellets fed to a RK reduction process, 665.57 kg carbon was consumed with 2437.99 kg CO_2 emissions. Those indices were 596 kg and 2396.11 kg, respectively, using the present technology. Approximately 10% of CO_2 emissions could be eliminated compared with a traditional RK reduction process.

Low-grade iron ores with high silica content are widely distributed in China, India, and Africa.[6,8,37] Moreover, over 7 billion tons of iron ore tailings (TFe ∼ 20 mass%, SiO_2 ∼ 75 mass%) are produced annually by the rapid development of the iron and steel industry in China.[5] Efficient utilization of these resources is of great benefit to the ironmaking and steelmaking industries in these areas. The present work may be helpful for researchers and process designers to enable efficient utilization of low-grade iron-ore resources.

CONCLUSION

1. A pilot-scale RK (Φ 1.5 m × 15 m) used for direct reduction of CPs can be divided into three major functional areas. In the 13.5- to 11.0-m zone (temperature range of 1023–1163 K), hematite was reduced to wüstite. The wüstite transformed to fine metallic iron particles within the 11.5- to 6.5-m zone (1163–1318 K). Metallic iron particles aggregated within the 6.5- to 0-m zone. Products with a metallization ratio of 92% were discharged from the RK.

2. Compressive strength of the CPs stabilized at 30–45 N during the reduction of hematite to wüstite. Formation and agglomeration of the metallic iron phase improved the strength to 468 N. The evolution of the strength characteristics was beneficial for avoiding disintegration of CPs in the RK.

3. Of the total iron present in this low-grade ore, 85.61 mass% was recovered in the form of iron powder (grade: 92.04 mass%), after the reduced product was treated by a magnetic separation process. Compared with oxidized pellets fed to an RK reduction process, approximately 10% of CO_2 emissions can be eliminated to produce 1 t pig iron using the present technology.

ACKNOWLEDGEMENT

The authors express appreciation to the National Natural Science Foundation of China (Grant No. 51504230) for financial support of this research.

REFERENCES

1. Y.S. Sun, Q. Zhang, Y.X. Han, P. Gao, and G.F. Li, *JOM* 70, 144 (2018).
2. V. Rayapudi and N. Dhawan, *Mater. Today: Pro.* 5, 17035 (2018).
3. G.H. Li, S.H. Zhang, M.J. Rao, Y.B. Zhang, and T. Jiang, *Int. J. Miner. Process.* 124, 26 (2013).
4. C.C. Yang, D.Q. Zhu, J. Pan, and L.M. Lu, *JOM* 69, 1663 (2017).
5. D.C. Fan, N. Wen, J.Y. Wang, and K. Wang, *J. Wuhan Univ. Technol. Mater. Sci. Ed.* 32, 508 (2017).
6. A.S.S. Ahmed, M.M. Eltahir, and M.A. Abdel-Zaher, *Int. J. Miner. Process.* 122, 59 (2013).
7. B. Kar, H. Sahoo, S.S. Rath, and B. Das, *Miner. Eng.* 49, 1 (2013).
8. S.S. Rath, D.S. Rao, and B.K. Mishra, *Int. J. Miner. Process.* 157, 216 (2013).
9. S.S. Rath, H. Sahoo, and B. Das, *Int. J. Miner. Metall. Mater.* 20, 605 (2013).
10. W. Yu, T.C. Sun, and Q. Cui, *Int. J. Miner. Process.* 133, 119 (2014).
11. W. Yu, T.C. Sun, and T.Y. Hu, *ISIJ Int.* 55, 329 (2015).
12. Y.S. Sun, Y.X. Han, P. Gao, Z.H. Wang, and D.Z. Ren, *Int. J. Miner. Metall. Mater.* 20, 411 (2013).
13. Y.S. Sun, Y.X. Han, P. Gao, and D.Z. Ren, *Int. J. Miner. Metall. Mater.* 21, 331 (2014).
14. R.Z.A. Rashid, S. Mohd, A. Hamzah, H.Y. Mohd, A.A. Nurul, and P.H. Tomohiro, *Renew. Energy* 63, 617 (2014).
15. A. Baikadi, V. Runkana, and S. Subramanian, *IFAC-Pap. Online* 49, 468 (2016).
16. K. Miura, K. Miyabayashi, M. Kawanari, and R. Ashida, *ISIJ Int.* 41, 1234 (2001).
17. M. Nakano, M. Naito, K. Higuchi, and K. Morimoto, *ISIJ Int.* 44, 2079 (2004).
18. Z.K. Liang, L.Y. Yi, Z.C. Huang, B.Y. Huang, and H.T. Han, *ACS Sustain. Chem. Eng.* 7, 18726 (2019).
19. Z.C. Huang, R.H. Zhong, L.Y. Yi, T. Jiang, L.M. Wen, and Z.K. Liang, *Metall. Mater. Trans. B* 49, 411 (2018).
20. Z.C. Huang, R.H. Zhong, J. Zou, and T. Jiang, in *6th International Symposium on High-Temperature Metallurgical Processing* (Springer, 2015), pp. 185–192.
21. Y. Man, J.X. Feng, Q. Ge, Y.M. Chen, and J.Z. Zhou, *Powder Technol.* 256, 361 (2014).
22. H. Park and V. Sahajwalla, *ISIJ Int.* 54, 49 (2014).
23. K. Sinha, T. Sharma, and D.D. Haladar, *Int. Eng. Adv. Technol.* 3, 30 (2014).
24. D.S. Chen, B. Song, L.N. Wang, T. Qi, Y. Wang, and W.J. Wang, *Miner. Eng.* 24, 864 (2011).
25. L.Y. Yi, Z.C. Huang, T. Jiang, R.H. Zhong, and Z.K. Liang, *Powder Technol.* 317, 89 (2017).
26. A.A. El-Geassy, M.I. Nasr, and E.A. Mousa, *Steel Research Int.* 81, 178 (2010).
27. Z.C. Huang, L.Y. Yi, and T. Jiang, *Powder Technol.* 221, 284 (2012).
28. Z.X. Zhang, X.J. Wu, T. Zhou, Y.S. Chen, N.P. Hou, and G.L. Piao, *Proc. Combust. Inst.* 33, 2853 (2011).
29. T. Jiang, G.Q. He, M. Gan, G.H. Li, X.H. Fan, and L.S. Yuan, in *Proceedings of the 5th International Congress on the Science and Technology of Ironmaking* (Shanghai, 2009), pp. 292–297.
30. Q. Zhong, Y.B. Yang, T. Jiang, Q. Li, and B. Xu, *Powder Technol.* 323, 195 (2018).
31. Q.M. Meng, R.F. Wei, J.X. Wei, P. Wang, Z.F. Gao, Z.X. Di, and H.M. Long, *ISIJ Int.* 58, 439 (2017).
32. A.P. Zambrano, C. Takano, M.B. Mourao, and S.Y. Tagusagawa, *Mater. Res.* 19, 1344 (2016).
33. Q. Zhang, Y. Li, and G.Y. Jia, *J. Clean. Prod.* 172, 709 (2018).
34. H. Suopajärvi, K. Umeki, E. Mousa, A. Hedayati, H. Romar, A. Kemppainen, C. Wang, A. Phounglamcheik, S. Toumikoski, N. Norberg, A. Andefors, M. Öhman, U. Lassi, and T. Fabritius, *Appl. Energy* 213, 384 (2018).
35. A. Hasanbeigi, M. Arens, and L. Price, *Renew. Sustain. Energy Rev.* 33, 645 (2014).
36. P. Mans, and D. Saayman, in *The Fifth Ilafa Direct Reduction Conference* (Saltillo, 1986), pp. 236–240.
37. F. Wu, J. Deng, B. Mi, Z. Xiao, J. Kuang, H. Liu, M. Liang, B. Liu, and P. Yu, *Powder Technol.* 356, 170 (2019).